Sustainable concrete: Design and testing

Jeanette Visser [1], Sandra Couto [2], Anoop Gupta [3], Iñigo Larraza Alvarez [4], Valle Chozas Ligero [4], Tiago Sotto Mayor [2, 5], Raffaele Vinai [6], Penny Pipilikaki [1], Alessandro Largo [7], Agnese Attanasio [7], Mike Chaolung Huang [8], Marios Soutsos [6]

[1] TNO, the Netherlands

[2] CeNTI, Portugal

[3] BASF, Germany

[4] Acciona, Spain

[5] EMPA, Switzerland

[6] Queen's University of Belfast, United Kingdom

[7] CETMA, Italy

[8] TBTC, Taiwan

Producing concrete with secondary raw materials is an excellent way to contribute to a more sustainable world, provided that this concrete has at least the same performance during its service life as concrete made with the primary raw materials it replaces. Secondary raw materials for Light Weight (LW) aggregates (rigid polyurethane foams, shredded tire rubber and mixed plastic scraps) have been combined with secondary raw materials for the binder (fly ash, slag and perlite tailings) making sustainable concretes that were investigated for their suitability as LW, highly insulating concrete for four different types of applications. Compliance to desired engineering properties (workability, setting time) was not always feasible: it was mostly the low workability of the mixtures that limited their application. Contrary to well established cements, steering the workability by adding water was not an option for these binders that rely on alkali-activation. Eight successful mixtures have been tested further. The results have shown that it is possible to produce a non-structural sustainable concrete with good mechanical and thermal insulation properties.
Design of concrete made with novel materials is currently not feasible without extensive experimentation as no design rules exist other than empirically derived rules based on traditional materials. As a radical different approach, a flexible concrete mix design has been developed with which the concrete can be modelled in the fresh and hardened state. The numerical concrete mix design method proves a promising tool in designing concrete for performance demands such as elasticity parameters and thermal conductivity.

1   Introduction

Producing concrete from secondary raw materials is an excellent way to contribute to a more sustainable world. This concrete then is required to have at least the same performance during its service life as concrete made with the primary raw materials it replaces. Secondary raw material based concrete with similar performance, further called sustainable concrete in this paper, saves not only primary raw materials and reduces the waste pressure on the environment, it also reduces Green House Gas emissions (GHG) and energy (e.g. Muller [2014], fib [2004]).

Secondary raw materials for aggregates require waste streams that are available in large enough quantities for a substantial replacement in the concrete (production) industry and pose a socio-economic problem. Within Europe these are, among others, shredded tyre rubber, polyurethanes and plastics. These can be used as Light Weight (LW) aggregates in concrete [Attanasio, 2015]. Their use as sustainable LW-aggregates in cement-based concrete is reported for rubber [Bravo 2012, Eldin, 1993, Fattuhi 1996, Sukontasukkul, 2006], polyurethanes [Mounanga, 2008, Perevozchikov, 2000, Václavík, 2012] and plastics [Choi, 2005, Jo, 2006, Lakshmi and Nagan, 2010, Marzouk, 2007, Pezzi, 2006, Rebeiz, 1996, Sikalidis, 2002] and were shown to improve the thermal insulating properties of concrete. Workability and compressive strength proved difficult to maintain [Eldin, 1993, Fattuhi, 1996, Sukontasukkul, 2006]. Similar results were found by [Attanasio, 2015] for tyre rubber, rigid polyurethane foams and recycled plastic scraps that are also used in this study.

Secondary raw materials such as fly ash, slag and perlite tailings are in sufficient large quantities available to serve as cement replacement [Vinai, 2015]. Sustainable binders, such as alkali activated fly ash, slag or combinations of these, have been shown to develop a higher compressive strength than a similarly composed concrete based on a Portland cement binder and gravel and sand as aggregates [Provis, 2014, Bernal, 2011]. Workability is more difficult to control as it depends on several parameters (e.g. activator type and concentrations) [Collins, 1999, Lee, 2013, Nath, 2014].

The current research focuses on designing concrete made with both secondary based binder and aggregate without negative impact on performance. Although the use of any of these materials in building products is not new [e.g. Sabnis, 2011], the combination of these sustainable materials to an all-waste type of concrete is. The aim of this paper is to report on the performance of concretes based on the combined use of waste aggregates and waste binders yielding a low weight, high insulating building material, with a low embodied energy, while maintaining its performance during its targeted service life of its building application. Results for both the fresh state and the hardened state are included. Durability tests are also part of the research but fall outside the scope of this paper and will be reported elsewhere. The carbon footprint of this sustainable concrete is reported in Gijlswijk [2015]. Full Life Cycle Analysis (LCA) and Life Cycle Costs (LCC) analysis will be reported at a later stage.

Combining sustainable LW-aggregate with a sustainable binder to a concrete that still has the same performance as a 'traditional' concrete, is quite a task. Most performance characteristics of hardened concrete (e.g. strength, thermal resistance) are impossible or not easy to design in advance and, in general, trial mixtures have to be made and tested to determine these properties [Flatt, 2012]. This is not a preferable way of concrete design when many different types of materials are available as it may result in extensive experimental programs to find (the most) suitable aggregate/binder combination and the optimum aggregate volume fraction. Moreover, these programs require reruns if the properties of one of the constituents changes since then also performances may change for the worst and even the most opportune combinations of aggregate/binder may change as well. The lack of research on concrete design methods other than consisting of large testing schemes is disconcerting. Optimization of sustainable concretes is still often sought by optimization of the aggregate packing, on the presumption that if the cement content can be lowered, the environmental impact will reduced [Mueller, 2014]. For the sustainable concrete in this research, no primary materials are used in the binder production so this assumption is not a priori valid. Moreover, by the use of LW aggregates, many performances such as strength will be reduced with a decrease of binder content [EuroLigthCon, 2008]. For this reason, a radical different approach from traditional concrete design has been sought in a modern way of concrete design. The second half of this paper is devoted to the principle of performance based design of sustainable concrete. The aim is to show how it can be used as a design tool.

2   Fresh concrete research

2.1   *Materials*

Binders

Three types of binders have been used in the research:

- cyclones and μ-silica, being wastes from a perlite production plant, in a 90/10 weight proportion and either activated by only NaOH solution (denoted as alkali activator) or using both NaOH solution and waterglass (denoted as WG activator);
- PFA, with NaOH / waterglass activation;
- PFA/GGBS mixture with various PFA/GGBS ratios and NaOH / waterglass activation.

All binders have been described in detail in Vinai [2015], including the concentration and type of activators.

Aggregates

Also three types of light weight (LW) aggregates have been used:

- Shredded rigid polyurethane foam (PU) (grades 0-4 mm and 4-8 mm);
- shredded tyre rubber (TR) (grades 0-0.6 mm, 0.6-2 mm, 2-4 mm, 3-7 mm);
- high density Remix (RX HD) (grades 0-3 mm and 3-7 mm): mixed plastic wastes obtained after sorting plastics from municipal solid wastes, combined with a low density Remix (RX LD) 8-12.5 mm grade. Gypsum was used as foaming agent to obtain the LD aggregates but the mixed plastic wastes are similar.

All aggregates have been described in detail in Attanasio [2015], including their production process. In addition to the LW aggregates, sometimes Natural Sand (NS) (grades 0-2 mm or 0-4 mm) was used as well.

2.2   *Target requirements*

The targeted mix designs were aimed for four types of application: floor screed, floor screed underlay, panel for facades and blocks. For these applications, a pre-described workability, density, and compressive strength were taken from the standards. The target requirements for different applications are mentioned in Table 1.

Table 1: Target requirements for different applications, compressive strength and density requirements at 28 days

Application	Workability	Compressive strength (MPa)	Density (kg/m³)
Floor screed	ready mix: ≥ 12.5/100 mm slump (60 min.)	≥ 5	<1100
Floor screed underlay	ready mix: ≥ 12.5/100 mm slump (60 min.)	≥ 8	<1100
Panels for facades	precast: ≥ 16/100 mm slump (30 min.) precast-SCC: ≥ 70/650 mm flow (30 min.)	5 - 20	<1500
Blocks	0-30 mm slump (15 min.)	≥ 5	1000-1400

2.3 Characterization methods

The workability of concrete was evaluated by slump, slump flow and spread measurements. The slump and slump flow were evaluated according to the EN 12350-2 standard. Spread measurement was performed according to the EN 12350-5 standard. The concrete density was evaluated according to the EN 12350-6 standard. The compressive strength was measured according to the EN 12390-3 standard.

Figure 1: Example of workability for cyclone / μ-silica with PU aggregates: 580 mm slump flow (after 4 min) and 100 mm slump (after 30 min)

2.4   Fresh concrete mix trials: initial design and compatibility , casting and curing issues

The initial design of the concrete was based on the (theoretical) density of concrete. All binder / aggregate combinations were tested, with the optimum binder compositions as formulated by Vinai [2015]. As most of the available aggregates reduced the workability, the biggest challenge in the fresh concrete design was to make the concrete as light as possible while maintaining a sufficient workability. Normally, workability can be steered by adding more water to the mix, using superplasticisers or adding some more round particles that can cause a lubrication effect. As the geopolymerization process is quite sensitive to the amount of water in the mix, adding water was not an option. In addition, especially for the PU aggregates with a density of only 330 kg/m^3, adding water may result in segregation if the viscosity of the mixture is reduced too much. Commercially available superplasticiser proved to be ineffective in these novel types of concretes, so that workability could be steered only by adding more round particles. For the PFA/GGBS binders, it was possible to add (more round) fly ash particles in the binder blend. For the other binders, the only possibility was adding sand, but this also increased the density of the mix. The amount of sand that could be added was therefore limited by the targeted density of the concrete.

Compatibility discrepancies between the aggregates and the binders may cause mixing and casting problems and, ultimately, poor quality of the concrete. Literature results showed that for both the used aggregates and binders, workability could be difficult to control [Eldin, 1993, Fattuhi, 1996, Sukontasukkul, 2006, Collins, 1999, Lee, 2013, Nath, 2014]. A quick assessment of the initially designed fresh concrete mixtures was therefore made firstly on the basis of workability. As two binders (the activated fly ash and cyclone/ μ-silica based binders) required heat curing to harden within a reasonable time span, also curing is an important stage for developing a good quality concrete. The (geo-) polymerization underlying the hardening of the activated fly ash and cyclone / μ-silica based binders is a two-stage process: in the first, dissolution and the formation of the monomers takes place, requiring water. The actual hardening takes place during the second stage (polymerization). During this stage, however, water should be able to escape [Vinai, 2015]. The effect of curing has been tested by compressive strength tests.

Different mixing, casting and curing approaches were also tried in this study. In general, mixing was started with the aggregates, adding the coarse particles first, followed by the (pre-blended) binders, and then (pre-blended and aged if required) liquids (water and

64

activators). After each step, mixing was executed to assure a good dispersion of the various components. Mixing times were adjusted by visual quality control. Casting was done either in plastic moulds or steel moulds, depending on preferences of the laboratory. Because of the adhesion issues between the geopolymers and the steel.

The major results of the mix trials were as follows:

- Despite different (re-)cleaning techniques, the 0/3 mm RX aggregates were rejected because this fraction caused heat formation, quick drying and swelling of the concrete. This was most likely caused by residual impurities such as metallic aluminium in the plastic waste stream [Attanasio, 2015].
- TR aggregates mixes gave rise to quick setting that could be overcome by additional mixing. The quick setting was likely flash set presumably due to a sudden reaction of sulphate compounds from the vulcanization process of tires, with the aluminium present in the binders.
- For the cyclones/µ-silica based binders, an optimized curing in two stages was developed: first curing at 70°C followed by a 55 °C curing to allow for the two-stage geopolymerization process. The durations of curing depended on the concrete composition and laboratory equipment. After carrying out the compressive strength tests, it was found that despite the high mass loss only the external layers of the samples were hardened and the internal part was still soft. This indicates that curing was not homogeneous and the polymerization in the interior not complete (see Figure 2). The effect of the thermal insulating LW-aggregates on the curing of these binders resulted in too long heat curing
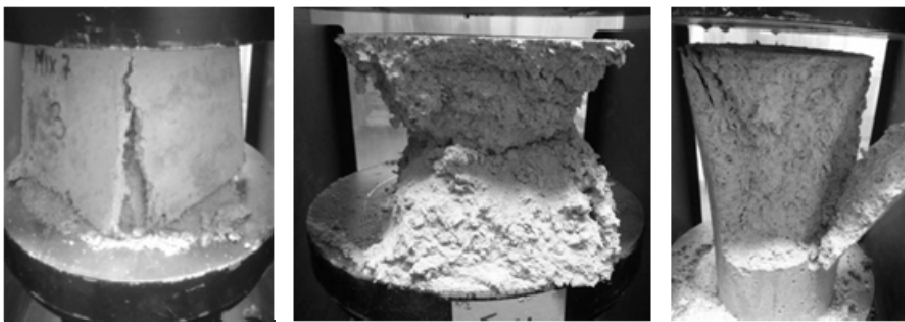

Figure 2: Disintegration of the specimen during the compression strength test showing that the interior of the specimens did not harden

regimes, even for the (relative) small specimens required for the mechanical testing. Therefore, these mixtures were further excluded from the research.

- To increase the geopolymerization rate in the PFA-binders, the moulds were oven-cured at 70 °C. It was found that the thermal expansion of the PU aggregates resulted in expansion of the specimen at young age, which resulted in low strengths (due to microcracking). Therefore, the curing regime was changed in a two stage curing procedure: first at 50 °C and then at 70 °C. The exact curing times depend on the type of laboratory equipment.

2.5 *Resulting fresh concrete mixes*

Based on the application requirements according to Table 1, further restrictions of the possible binder / aggregates combinations were as follows:

- for the floor screed and floor screed underlay, only the PFA/GGBS binder could be used as heat curing for these applications is not possible;
- workability of PU/PFA mixtures decreased rapidly over time. Contrary to cement which is known to have a dormant period during its hydration process [Neville, 2002], geopolymers do not. Hence, the so-called open time or workability window, i.e. the timeframe in which a mix can be placed and if required compacted, can be quite brief. This was the case for the PU/ PFA mixes. The workability window required for (the) facade panel was not achieved, and only block production was targeted for these mixes;
- compared to the PFA-binder mixtures, lower volume fraction of aggregates had to be used in the PFA/BGGBS-binder mixtures. All used aggregates reduced the workability considerably and GGBS does not improve the workability the same way as PFA does, among others due to its more angular shape in comparison to the well-rounded PFA particles [Vinai, 2015]. Also for these binder mixtures, replacement of sand in the mix increased the workability drastically. At the same time this increased the density frequently above its target so that sand replacement was not an option. Therefore, the PFA/GGBS ratio was sometimes increased.

The best mixtures for the PFA-binders are shown in Table 2; those for the PFA/GGBS-mixtures in Table 3. Sometimes the workability could not be measured at the required time due to practical constraints, e.g. the time elapsed before the slump test could be executed.

Figure 3: Example of workability for PU/PFA showing slump flow after 4 min.

As the workability decreases with time, a higher workability at later times was generally considered acceptable for the facade and screed applications. For blocks, the reverse applies since these are stamped and need to be demoulded immediately. In this case a lower slump is allowed. For TR/PFA combinations, no mixtures could actually be found that fulfilled all requirements (Table 2). The best one has been included in the experimental program.

For screed application (only PFA/GGBS mixtures), the workability requirements could not be guaranteed for 60 minutes for any combination (Table 3). Neither could the workability

Table 2: Resulting PFA binder concrete: fresh concrete workability and density and strength of the hardened concrete at 28 days (see Annex A for quantities); aggregates as volume proportion of the concrete and targets between brackets

Mix no.	Aggregate (fraction)	Workability (slump in mm) / time (min) (target)	Density (kg/m^3) (target)	Strength (MPa) (target)	Application
2_1	PU + sand 60%	25 / 25 (0-30 / 15)	1230 (1000-1400)	5.1 (> 5)	block
2_2	PU 50%	30 / 20 (0-30 / 15)	895 (1000-1400)	5.6 (> 5)	block
2_3	TR + sand 50%	90 / 15 (0-30 / 15)	1460 (1000-1400)	4.6 (> 5)	block
2_4	RX + sand 45%	170 / 20 (≥ 160 / 30)	1430 (<1500)	5.9 (5-20)	panel for facades

Table 3: Resulting PFA/GGBS binder concrete: fresh concrete workability and density and strength of the hardened concrete at 28 days (see Annex A for quantities); aggregates as volume proportion of the concrete

Mix no.	Aggr. (fract.)	Binder	Target workab. (slump)	Workab: slump (mm)	Density (kg/m³) (target)	Streng. (MPa) (target)	Appl.
3_1	PU 45%	PFA/GGBS 75/25	ready mix: ≥ 125/100 (60 min)	180 (30 min.)	1090 (<1100)	8.4 (> 8)	floor screed underlay
			ready mix: ≥ 125/100 (60 min)	180 (30 min.)	1090 (<1100)	8.4 (>5)	floor screed
			Precast: ≥ 160/100 (30 min.)	180 (30 min.)	1090 (<1100)	8.4 (5-20)	panel for facades
3_2	PU 45%	PFA/GGBS 85/15	Precast-SCC: flow ≥ 70/650	525 (30 min.)	1210 (<1500.)	7.6 (5-20)	panel for facades
3_3	PU 45%	PFA/GGBS 15/85	0-30 (15 min.)	10 (15 min.)	1165 (1000-1400)	15.1 (> 5)	block
3_4	RX 40%	PFA/GGBS 50/50	0-30 (15 min.)	25 (15 min.)	1475 (1000-1400)	18.2 (> 5)	block

of the precast SCC for facades be achieved. The PU/PFA/GGBS mix (mix 3_1) was found to be the best mix meeting the density and compressive strength requirements and having good workability (180 mm after 30 min.). The PU/PFA/GGBS (mix 3_1) is also suitable for facades precast applications. For blocks application, where low initial workability is needed, binder blends with a low PFA/GGBS ratio (50/50 and 15/85) could be used.

A concrete mix with PFA/GGBS binder and RX aggregates for the block application has been added in the experimental program although the density slightly exceeded the target. This mix proved to be the optimum mix. Increasing the aggregate fraction to reduce the density resulted in an inhomogeneous mixture, mixes with decreased PFA/GGBS ratio set before 15 minutes, while mixes with increased PFA/GGBS ratio resulted in workability higher than 30 mm after 15 minutes.

3 Hardened concrete research

3.1 *Test program and results*

The performance of the eight mixtures in Table 2 and Table 3 were tested further according to the test program in Table 4. Table 5 summarizes the results.

Table 4: Test program for the hardened concrete

Test	Dimensions specimens (mm)	Number of specimens	Standard
Compressive strength	100 x 100 x 100	3	EN 12390-3
Young's modulus	50 x 100	2	UNI-EN 6556
Flexural strength	400 x 100 x 100	2	EN 12390-5
Thermal conductivity	150 x 150 x 70	2	EN 12664

Table 5: Summary of the experimental results on the hardened concrete at 28 days, full mix compositions are given in Annex A, aggregates as volume proportion of the concrete, mix 3_2 has been cast in two-fold. Notation: f_c = compressive strength, f_{flex} = flexural strength, E = Young's modulus and λ = thermal conductivity

Mix no.	Aggregate	Binder	Density (kg/m³)	f_c (MPa)	f_{flex} (MPa)	E (GPa)	λ (W/mK)
2_1	PU+s 60%	PFA	1300	8.3 ± 0.0	2.0 ± 0.1	1.9 ± 0.3	0.31
2_2*)	PU 50%	PFA	895	5.6 ± 0.2	1.2 ± 0.1	1.1 ± 0.2	0.16
2_3*)	TR+s 50%	PFA	1490	4.2 ± 0.1	0.9 ± 0.1	0.9 ± 0.3	0.32
2_4	RX+s 45%	PFA	1530	6.8 ± 0.3	1.3 ± 0.2	1.0 ± 0.1	0.34
3_1	PU 45%	PFA/GGBS 75/25	1145	8.4 ± 0.1	1.4 ± 0.1	0.9 ± 0.1	0.18
3_2a	PU45%	PFA/GGBS 85/15	1115	6.2 ± 0.0	0.8± 0.0	1.1 ± 0.4	-
3_2b	PU45%	PFA/GGBS 85/15	1025	6.6 ± 0.1	0.9 ± 0.0	-	0.17
3_3	PU 45%	PFA/GGBS 15/85	1165	15.1 ± 0.0	2.1 ± 0.2	3.1 ± 0.2	0.20
3_4	RX 40%	PFA/GGBS 50/50	1475	18.2 ± 0.0	2.3 ± 0.3	3.4 ± 0.2	0.27

The failure mode for mixes with PU aggregates (e.g. mix no. 3_3 in Figure 4) can be classified as very brittle: after reaching the peak stress, the stress immediately dropped to almost zero. The concrete with the TR aggregates (mix no. 2_3 in Figure 4) showed a slightly more ductile behavior. RX samples had an intermediate behavior. The softening behavior is mostly driven by the aggregates and not by the binder, as both PFA and PFA/GGBS matrix failures are typically brittle. It was observed that TR grains did not crush but first deformed and next were pulled out (likely by friction-slip) from the matrix. For the PU aggregates, the fracture ran through the aggregates. RX aggregates showed an intermediate behavior: sometimes the cracks ran through the aggregates, but the plastic shreds within the aggregates prevented complete failure of these aggregates.
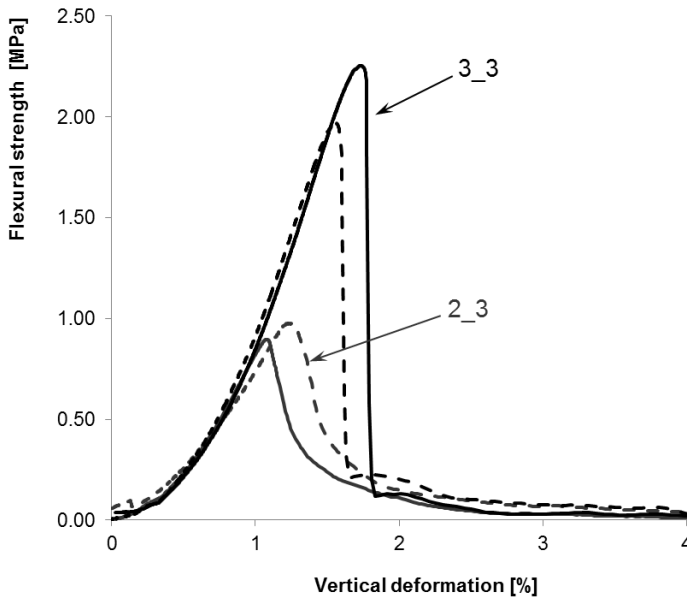
Figure 4: Test curves for 3_3 (PFA/GGBS and PU 45%) and 2_3 (PFA and TR+s 50%) samples; dashed and solid lines are indicating tests on different specimen.

3.2 Mechanical behavior as compared to normal LW concrete

Concrete is designed solely on compressive strength as indicator of the mechanical performance. All other mechanical properties (e.g. tensile strength) are related to this compressive strength in the building codes or the Fib Model Code 2010 (being destined to become the next generation building codes). It is generally assumed that if the mechanical relations in the building codes also hold for the new types of concrete, it becomes plausible

70

that also all relating failure mechanisms with respect to the mechanical loads in the Fib Model Code 2010 are fulfilled as well. This assumption is based on the similarity in inorganic binder composition, resulting in the same type of mechanical behavior. For a more extensive reading on this topic, see [Visser and Bigaj, 2014].

To investigate whether a similar relationship may be applied for the developed sustainable concrete as for already accepted LW concrete defined in the Fib Model Codes 2010 for concrete grades $\leq$ C50, the tensile strength of the developed sustainable concrete should fulfil the following set of relations:

$$
\begin{aligned}
f_{ctm} &= 0.3\,\eta_l\,(f_{ck})^{2/3} \\
f_{ctk,\min} &= 0.7\,f_{ctm} \\
f_{ctk,\max} &= 1.3\,f_{ctm}
\end{aligned}
\tag{1}
$$

where f_{ctm} is the calculated tensile strength, f_{ck} is the characteristic compressive strength, $f_{ctk,\min}$ and $f_{ctk,\max}$ are the lower and the upper bound values of the characteristic tensile strength, respectively. For light weight concrete, a reduction factor η_l is included:

$$
\eta_l = 0.4 + 0.6\frac{\rho}{2200}
\tag{2}
$$

in which ρ is the oven dry density of the aggregate (in kg/m³) being on average 330 kg/m3 for PU, 970 kg/m³ for TR and 810 kg/m³ for RX.

The characteristic compressive strength has been calculated on the basis of a 10% variance, since the standard deviations in the tests were only based on three tests and too low to make a good assessment of the standard variation for the population possible. Also, due to the low strengths, a constant standard variation of 8 MPa could not be used in this case. As the tensile strength has been measured by means of a four point bending test, the correction factor to include is:

$$
f_{ctm} = \alpha_{lf}\,f_{ctmfl}\,,
\tag{3}
$$

where:

f_{ctmfl} is the mean flexural tensile strength;

$$
\alpha_{lf} = \frac{0.06\,h_b^{0.7}}{1 + 0.06\,h_b^{0.7}}
$$

h_b is the beam depth (100 mm in these tests).

Figure 5 shows the comparison between the measured flexural tensile strength and that calculated from the compressive strength according to the above relations. As can be seen, with the exception of the mix 2_1 the relationship holds also for the developed sustainable concrete. For mix 2_1, measured flexural tensile strength is much higher than the predicted one on the basis of the compressive strength. There is no indication what has caused this. For all other combinations, including other PFA/PU mixes, the relation between measured flexural tensile strength and compressive strength as given in the Fib Model Code 2010 is applicable.

The modulus of elasticity for lightweight concrete Elci can be estimated from the following equation according to the Fib Model Code 2010:

$$E_{lci} = \eta_E E_{c0}(\frac{f_{cm}}{10})^{\frac{1}{3}}$$
(4)

with $\eta_E = (\frac{\rho}{2200})^2$ and ρ is the oven dry density of the lightweight aggregate concrete in kg/m³ (being on average 330 kg/m³ for PU, 970 kg/m³ for TR and 810 kg/m³ for RX, as
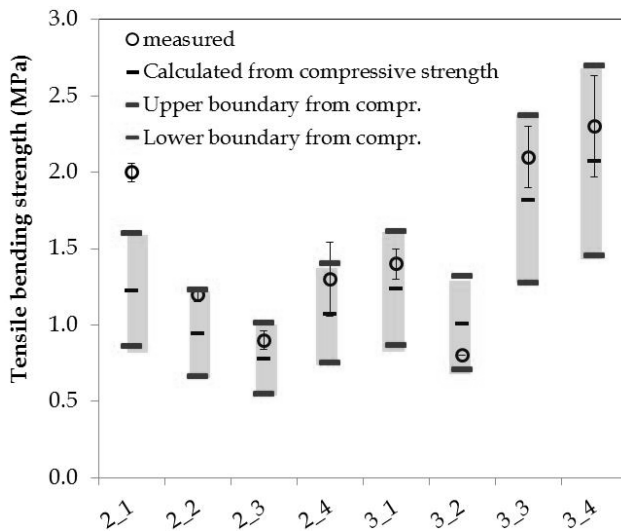

Figure 5: Comparison between measured flexural tensile strength and predicted compressive strength according the Fib Model Code 2010; coding of the mixtures according to Table 5

72

also used for the tensile bending strength), Eco = $21.5 \cdot 10^3$ MPa and f_{cm} is the mean compressive strength (MPa).

In Figure 6, the measured and predicted Young´s moduli are shown. Although no upper and lower boundaries are given in the Model Code 2010 for the Young's moduli, the same upper and lower boundaries are used as for the tensile bending strength, namely the 0.7 and 1.3 times the calculated value.

Figure 6 shows that all PU-mixtures have a measured Young's modulus higher than the predicted one on the basis of eq. (4), whereas for the other aggregates, the combination with PFA binder resulted in lower values than predicted. Only for the RX with the PFA/GGBS, the prediction proved to be good.

3.3 Achieved thermal conductivity

The results obtained regarding thermal conductivity (Table 5) show λ-values from 0.16 W/mK (PU/PFA) to 0.34 W/mK (RX/PFA). As the LW aggregates have a very low thermal conductivity themselves (0.04 W/mK for TR and 0.06 W/mK for PU, no reliable data for RX available), the thermal conductivity of the SUS-CON concrete decreases
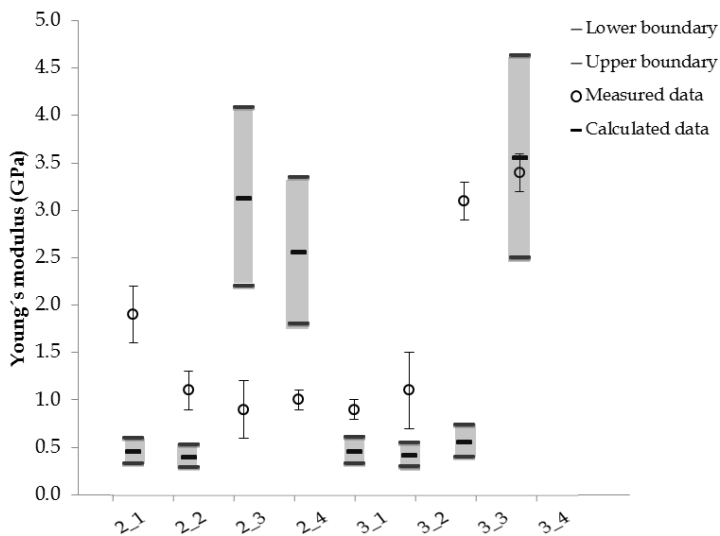

Figure 6: Comparison between measured and predicted Young´s modulus; coding of the mixtures according to Table 5

considerably with these LW aggregate fractions. The addition of sand, having a thermal conductivity of circa 4.8 W/mK, adversely affects the thermal insulation capacity.

3.4   *Possible applications for the SUS-CON concrete*

In Table 6, a comparison is made between the performance demands and the obtained results for the newly casted specimens in the hardened concrete research. As discussed in

Table 6: *Compliance of the hardened concrete with the performance demands for various applications; densities and compressive strength are based on different specimens from the fresh concrete tests of Section 3*

Mix selected			Compliance with application				
Mix no.	Aggregate	Binder	Target density (kg/m³)	Measured density (kg/m³)	Target f_c (MPa)	Measured f_c (MPa)	Application
2_1	PU+s 60%	PFA	1000-1400	1300	≥ 5	8.3 ± 0.0	block
2_2	PU 50%	PFA	1000-1400	895	≥ 5	5.6 ± 0.2	block
2_3	TR+s 50%	PFA	1000-1400	1490	≥ 5	4.2 ± 0.1	block
2_4	RX+s 45%	PFA	<1500	1530	5-20	6.8 ± 0.3	panels
3_1	PU 45%	PFA/ GGBS 75/25	<1100	1145	≥ 8	8.4 ± 0.1	floor screed (underlay)
			<1500	1145	5-20	8.4 ± 0.1	panels
3_2a	PU45%	PFA/ GGBS 85/15	<1500	1115	5-20	6.2 ± 0.0	panels
3_2b	PU45%	PFA/ GGBS 85/15	<1500	1025	5-20	6.6 ± 0.1	panels
3_3	PU 45%	PFA/ GGBS 15/85	1000-1400	1165	≥ 5	15.1 ± 0.0	block
3_4	RX 40%	PFA/ GGBS 50/50	1000-1400	1475	≥ 5	18.2 ± 0.0	block

section 2, the balance that had to be found in the concrete design was to have a mix as light as possible (brought about by a high LW aggregate volume) while having strength as high as possible along with the desired workability (brought about by a high paste volume). An exception was represented by the blocks, where an almost zero workability is required, and thus the lightness and workability were affected in the same way in the mix design, rather than the strength and workability. Only in the case of TR/PFA the sample did not reach either target. This is in accordance with previous analyses in which those materials prepared with TR aggregates showed low compressive strengths. Low adhesion between the TR aggregates and the matrix makes it difficult for these aggregates to reach good strengths, especially at high aggregate fractions where non-bonded zones around the aggregates are likely to connect. As a conclusion, it can be said that the TR aggregates cannot be used in the combination of the binders tested for the targeted LW-applications. Thus, it can be concluded that only the PU aggregates were suitable for the applications under consideration. Together with the PFA they are applicable for blocks, whereas with PFA/GGBS blends they are also applicable for panels.

It has been mostly the low workability of the mixtures that has limited their application. Contrary to well established cements, steering the workability by adding water was not an option for the investigated binders. Adding sand was an option for the PFA-binders but not for the PFA/GGBS-binders as the density then increases above the target. For the binders in combination with the aggregates, no suitable additives could be found that were commercially available to improve the workability within this project.

4 Numerical concrete design for performance prediction

4.1 Basic principle of the modelling

From the previous sections, it has become clear that it requires quite an effort to design concrete with sustainable aggregate/sustainable binder, even on only two performance demands. Each additional performance demand and each new material considered will increase the experimentation scheme considerably. Without help of a design tool, all compositional design may therefore be sub-optimal. However, there is a lack of research on concrete design methods other than consisting of large testing schemes or optimization of the aggregate packing [Mueller 2014]. To develop an efficient way of designing concrete mixtures, a design tool has been developed. The design tool is based on the principle that the properties of concrete (and other composite materials) are determined by the properties

of the constituents, their volume fractions in the material and their spatial arrangement. Whereas the properties of the constituents in general can be determined separately, and the volume fractions are known when a concrete mix is designed, the spatial arrangement of the particles is difficult to predict. Moreover, the dependency on the spatial arrangement of most properties is different. For instance, the density of concrete is independent of the spatial arrangement of coarse aggregates in the mortar (consisting of cement paste and fine aggregates). In contrast, the thermal conductivity depends on the spatial arrangement.

In the literature, a whole range of different geometrical arrangements can be found to predict concrete properties that are dependent on the spatial arrangement of its constituents [Carson, 2005], ranging from simple parallel and series ordering of its constituents without considering the particle structure nor placement (Figure 7) to more advanced spatial arrangements. Although approximate models can be used as a first guess, they generally do not have sufficient predictive capacity for concrete design. The dependence of the concrete properties on the particles arrangement requires more detailed modelling.
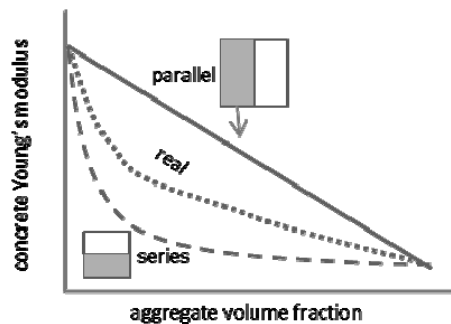

Figure 7: Schematized influence of the aggregate volume fraction on the Young's modulus of concrete for parallel, true and series arrangement of the aggregates

Discrete element method (DEM) is becoming widely accepted as an effective method of addressing engineering problems in granular materials, as proven by Stroeven [1999] and continued research based on this work (see e.g. He [2010, 2012], Stroeven [2015]). Stroeven [1999] has shown that all types of concrete compositional defects also can be simulated with this method, such as wall effects around aggregates (giving rise to porous interfaces

and thus low strengths) and inefficient packing (giving rise to high porosity and thus also low strength and durability).

In line with the goals of this research, the concrete has been modelled as a two phase material consisting of mortar and coarse aggregate. Hence, the mortar has been modelled as one phase or constituent, consisting of the binder(s), small aggregates with a diameter up to 2 mm, water and additives. Testing mortars to determine the properties of the binders for concrete composition design is standard practice: standard strengths of cement, for instance, are determined on such a mortar. From the numerical point of view, some practical issues can be avoided in this way as well. Although it is possible to model a large size range of particles of various shapes, discrete element methods are relatively computationally-intensive, with computational times increasing fast with the number of aggregate size classes included and higher packing densities. The validity of this phase separation, also called scale separation, has not yet been proven beyond doubt, but is required to restrict computer efforts.

Most mortars/concretes develop their properties over time due to ongoing hydration/chemical reactions after mixing the binders with water and possibly activator. The properties of the mortar were measured as a function of time, which renders possible predicting time dependent properties of the mortar. This method was chosen over simulation of the time dependent chemical hydration reactions because of the uncertainty in reaction products in this research (e.g. Hymostruc [Breugel, 1991], CEMHYD3D [Bentz, 2005], μic [Bishnoi and Scrivener, 2009], XIPKM [Le, 2013]).
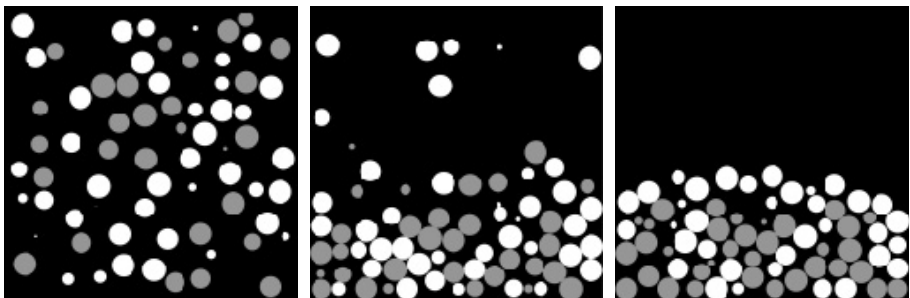

Figure 8: Evolution of particle packing showing segregation phenomena, for particles with different densities – lighter (white) particles fall slower than heavier (grey) particles

Modelling

The open software tool LIGGGHTS [Kloss, 2012] used in the present work involves a random sequential addition (RSA) step in which particles are sequentially placed in random positions in a container followed by a DEM step to predict the evolution of particle positions taking into consideration the particle-particle and the particle-fluid interactions.

After initial placement of the particles in a container, the rearrangement of the particles needs to be modelled. For the current simulation, no stirring or shaking has been included. Fluid – particle forces included were the buoyancy force and friction (drag force) of fluid on the particles. The buoyancy force depends on the fluid density and the particle size, according to:

$$F_{buoyancy} = \rho_{fluid} \left(\tfrac{4}{3} \pi R_{particle}^3\right) g \; , \tag{5}$$

where ρ_{fluid} is the fluid density, $R_{particle}$ is the particle radius and g is the gravity acceleration. The drag force depends on the behaviour of the fresh mortar, according to:

$$F_{drag} = C_{drag} \, 6 \pi \mu \, R \, v \; , \tag{6}$$

where v is the velocity (of the particle moving through the fluid), R is the particle radius, μ is the fluid viscosity and C_{drag} depends on the constitutive equation of the fluid.

The particle-particle interactions were calculated based on the contact geometry [Fennis, 2011, He, 2010, Kloss and Goniva, 2012, Stroeven, 1999] and described by Coulomb's law of friction and both normal (contact and damping) and tangential (shear and damping) forces were considered.

The fresh mortar behaves as a Bingham fluid but only in its dormant period. After this period the cement hydration/alkali-activated binder reactions become relevant and the mortar can no longer be modelled as a Bingham fluid. Thus, after the dormant period, the drag force is not modelled accurately anymore (Figure 9). For the majority of the mixes, placement of the aggregates will be finished well before the mix stiffens due to hydration. Mixtures which will 'solidify' before settling completely are unlikely to be used in practice because of their low open time. On the other hand, if workability is too high, it is possible
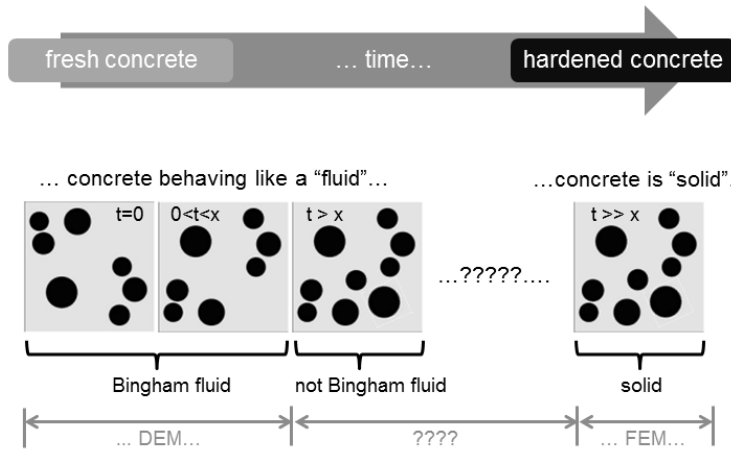
Figure 9. Simulation approaches to study concrete performance

that unwanted phenomena such as segregation or bleeding can occur. Such phenomena can be predicted by DEM and some (virtual) mix modifications can made in order to avoid these phenomena (e.g. changing aggregate grading or density , changing the viscosity of the 'fluid' (the mortar) etc.).

Measuring the input material parameters in the model

The fresh mortar is described in the model as a Bingham fluid, characterized by the fluid viscosity, µ, and yield stress, τ_0 . To validate this choice of the constitutive equation for the mortar as well as to determine the input parameters for the numerical predictions, viscosity experiments have been performed on the (fluid) mortars. An example of the results is given in Figure 10. Together with the density, the fluid phase is fully described.

The mechanical interactions between the aggregates are defined by their elasticity parameters and two interaction coefficients: the coefficients of friction and of restitution, taking into account the loss of energy upon collision [Kloss and Goniva, 2012, Stroeven, 1999] . It was concluded from a sensitivity analysis of the modelling that, for the materials under consideration, the simulation results were not sensitive to the coefficient of restitution, therefore this coefficient was not measured. The coefficient of friction was measured by a classical Newtonian friction experiment by means of a simple tribometer, while the elasticity parameters were measured by means of Ultrasonic Pulse Velocity both

in the P- and S-mode. A summary of the required input with respect to the material properties is given in Table 7.

Simulations

The sustainable concrete mix has been simulated as discussed for a two phase-material consisting of coarse aggregates and a (fluid) mortar. The aggregate particles are inert, solid inclusions. For the sake of simplicity, only spherical particles were considered in the present study. For the LW concrete under consideration, optimum packing is not a design criterium. Instead, the maximum amount of aggregates that can be accommodated while still complying the strength demand (Section 3) is of more importance. In the simulation, the properties of the concrete are determined for volume fractions of the coarse aggregates in the range 0.1 to 0.38, the latter volume fraction being similar to total aggregate fraction around 0.7 when including the sand from the mortar. The aggregate particles size distribution was taken according to Fuller [Neville, 2002], with average particle sizes for the classes 2-4 mm, 4-8 mm and 8-16 mm. As an example, three particle packing simulations are shown in Figure 11, with coarse aggregate volume fractions of aggregate of 0.1, 0.3 and 0.38. Periodic boundaries were used.
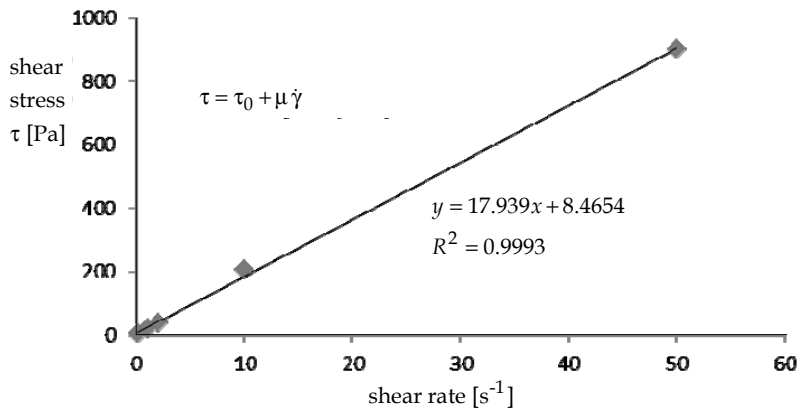

In the chart:

$$\tau = \tau_0 + \mu \dot{\gamma}$$

$$y = 17.939x + 8.4654$$
$$R^2 = 0.9993$$

shear stress τ [Pa] (y-axis), shear rate [s^{-1}] (x-axis)

Figure 10: Results of the viscosity experiments for the reference mortar, showing perfect Bingham fit

Table 7: Constituent properties required in the fresh state modelling

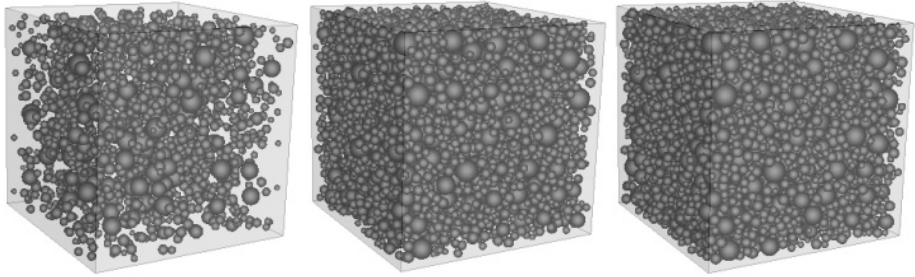| Particles properties	Fluid properties
Young's Modulus (GPa)	Density (kg/m³)
Poisson's ratio (-)	Viscosity (Pa s)
Coefficient of friction (-)	Yield stress (Pa)

Figure 11: Particle packing with different volume fractions of coarse aggregate (left to right: 0.1, 0.3 and 0.38 at equilibrium); container of 160 x 160 x 160 mm³ (tenfold the size of the largest particle)

In the example shown in Figure 11, the distribution of the particles at equilibrium can be seen to have remained well dispersed, contrary to the particles shown in Figure 8, which not only sank to the bottom of the container but also segregated. Although the density of the aggregates in Figure 11 is about 1.65-fold larger than that of the fluid mortar, the buoyancy force is not sufficient to overcome the critical yield. As a consequence, the particles remain well distributed even at these low coarse aggregate volume fractions where the aggregates settle in the mortar (and not settle at the bottom or drift to the top of the container).

4.3   *Hardened concrete state*

Modelling

The final, equilibrium condition of the DEM simulations as shown in the examples in Figure 11, is assumed to represent the particles in the hardened state, because the placement of the aggregates is finished, presumably well before the hardening or hydration process renders the particles immobile. It thus serves as input for the following simulation phase, addressing the performance of the hardened concrete, by a 2D FEM (Finite Element Modelling) approach. For this purpose, 2D sections of each 3D particle packing were extracted from the cross section in the middle of the simulation domain. The 2D sections resulting from the particle packing of Figure 11 are shown in Figure 12. For each property, boundary conditions were chosen in accordance with their definition in the constitutive equations. This means that the elasticity parameters of the concrete were calculated by simulating an uniaxial compression test (Figure 13 left), and the Young's modulus and Poisson's ratio were calculated according to their definitions by Hooke's law [He, 2010]. In a similar way, the thermal conductivity of concrete $k_{concrete}$ was calculated using the Fourier law in unidirectional steady-state heat transfer (Figure 13 right).

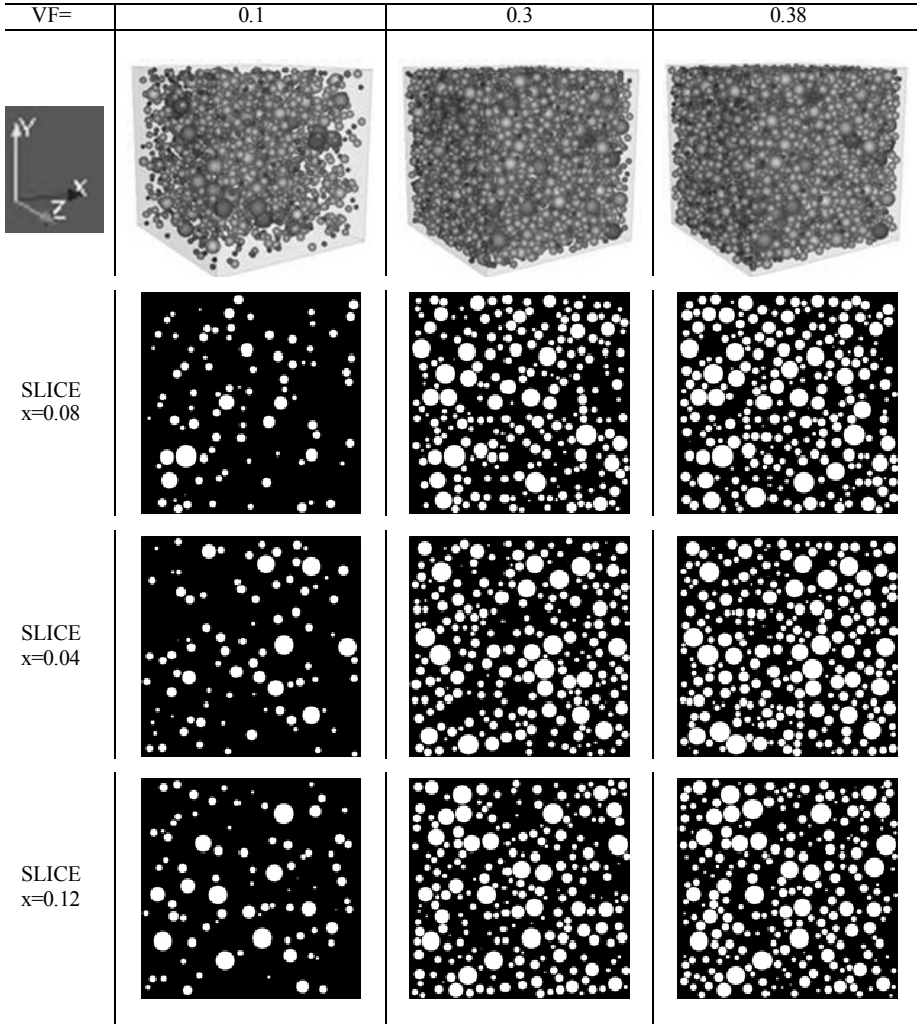| VF=	0.1	0.3	0.38
SLICE x=0.08			
SLICE x=0.04			
SLICE x=0.12			

Figure 12: Particle packings at three different coarse particle volumes of 0.1, 0.3 and 0.38 (top row) and cross-sections of the particle packing at three different locations (rows below)

Measuring the input material parameters

Each concrete parameter to be determined requires its own set of input parameters. For the elasticity parameters of the concrete, these are the two elasticity parameters (i.e. Poisson's ratio and Young's modulus) of the two constituents (coarse aggregates and mortar). For the thermal conductivity of the concrete, the thermal conductivity of the constituents is necessary. Thus, the elastic properties of the concrete constituents have been measured by
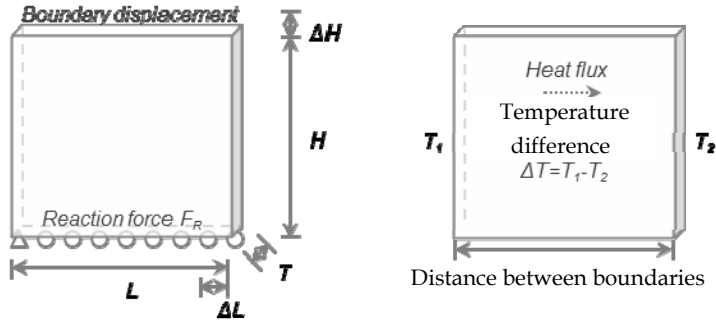
82

Figure 13: Boundary conditions applied for obtaining the Young's modulus (left) and the thermal conductivity (right) of concrete

means of UPV for P-waves and S-waves. The thermal conductivity of the mortar was determined according to EN 12664. For the aggregate, only an estimate could so far be obtained by compacting the loose aggregates in the hotplate equipment according to EN 12667. As the mortar is developing its properties over time, the elasticity parameters and the thermal conductivity have been measured at different ages. Figure 14 shows the age-dependency of the Young's modulus as an example. Table 8 shows the required properties of the constituents of the hardened concrete for the determination of the elasticity and thermal conductivity.

Simulations

A systematic numerical study was conducted in which the Young's modulus and thermal conductivity of the aggregate particles and the mortar were varied, while the remaining properties were kept constant. As an example, results for the Young's moduli are shown in Figure 15.
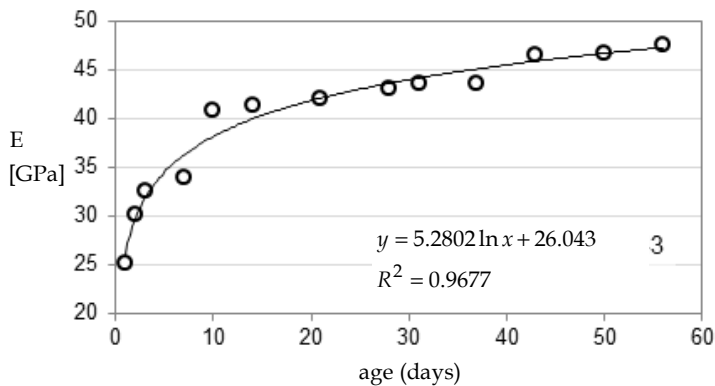

$$y = 5.2802 \ln x + 26.043$$
$$R^2 = 0.9677$$

Figure 14: Dynamic Young's modulus for various ages of the reference mortar

Table 8: Constituent properties required in the hardened state modelling

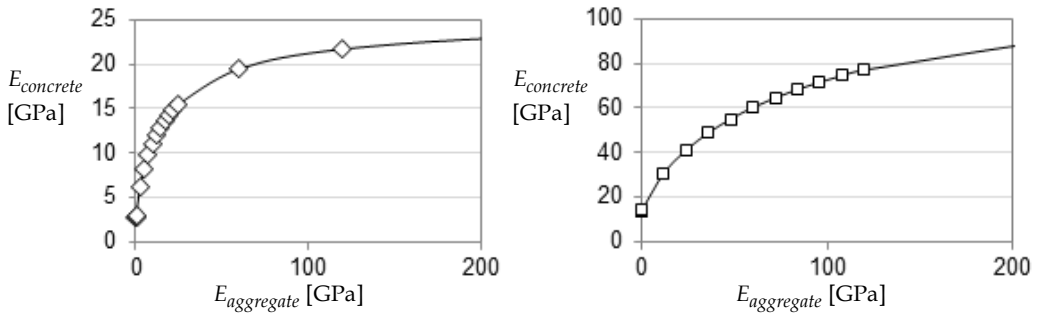| Coarse aggregate properties	Unit	Mortar properties (as function of age)	Unit
Young's Modulus	GPa	Young's Modulus	GPa
Poisson's ratio	-	Poisson's ratio	-
Density	kg/m³	Density in hardened state	kg/m³
Thermal conductivity	W/mK	Thermal conductivity	W/mK

Figure 15: Young's modulus of the concrete $E_{concrete}$ as a function of the Young's modulus of the aggregate $E_{aggregate}$, for E_{mortar} = 12 GPa (left) and for E_{mortar} = 60 GPa (right), volume fraction of aggregate = 0.38

As shown in Figure 15, when the aggregates have no stiffness and can be viewed as infinitely compressible (i.e., as 'air'), the stiffness of the concrete is reduced as compared to that of the mortar. When the aggregate stiffness is larger than that of the mortar, the stiffness of the concrete is increased. If the aggregates become however much stiffer than the mortar, further increase in stiffness has little effect as only the mortar deforms noticeably. At this stage, a final stiffness of the concrete is reached (Figure 16).

4.4   Design demonstration of the sustainable concrete

As a demonstration of its design possibilities, the properties of concrete have been calculated for concrete consisting of a reference mortar with either gravel or polyurethane foam (PU) as coarse aggregates. The results at 25% and 50% coarse aggregate fractions are shown in Table 9 (the 50 % PU is comparable to mix 2_1, although there is much less sand in mix 2_1).

The DEM/FEM simulations show that a quick numerical design for the various types of concrete investigated herein can be realized for elasticity and thermal insulation properties. The design can be extended to other properties that can already be simulated with related numerical models (e.g. Le [2014]). Although there is in general a good relation between viscosity of a mix and the workability (see e.g. Banfill [2006]), and recently, progress has been made in predicting the workability by a similar DEM-approach [Mechtcherine, 2015], the choice of a good workability reference method and the numerical validation of these practical test methods are still challenging.
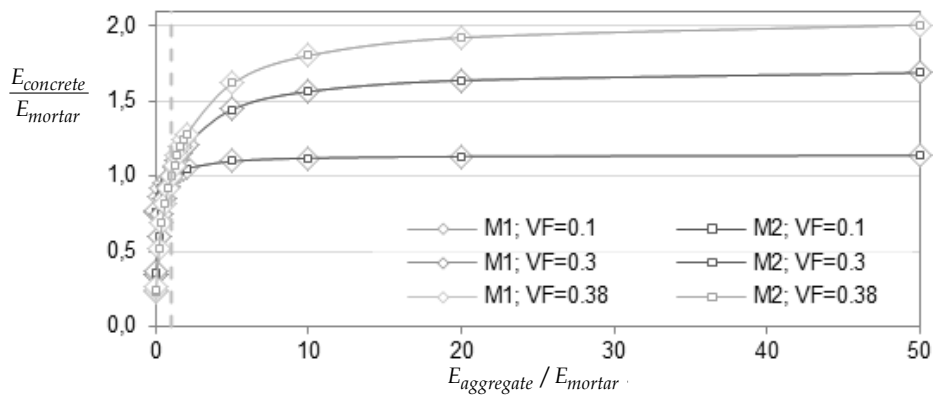

Figure 16: Young's modulus of the concrete (Econcrete) as a function of the Young's modulus of the aggregate (Eaggregate), both normalized by the Young's modulus of the mortar (Emortar), for two mortars (M1 and M2, characterized by Emortar of 12 GPa and 60 GPa, respectively) and for volume fractions of aggregate (VF) of 0.1, 0.3 and 0.38. Mortar curves M1 and M2 are the same, and only depending on the volume fraction of aggregates and mortar

Table 9: Simulated properties of concrete – replacing coarse gravel with PU

	Density	Young's Modulus	Poisson's ratio	Thermal conductivity
	kg/m^3	GPa	-	W/(mK)
PU 25%	1825	18.1	0.25	0.40
PU 50%	1326	3.4	0.23	0.12
Gravel 25%	2405	44.4	0.20	0.96
Gravel 50%	2486	57.0	0.15	2.05

5   Conclusions

In this research toward new types of sustainable concrete, the fresh concrete mix trial in which the workability was investigated in relation to the aggregate volume fraction showed that combing the geopolymeric binders with the new types of aggregates could lead to compatibility problems such as gas formation, extreme heat formation, corrosion of the moulds and flash- and fast set. Heat curing in relation with the thermal low conductive aggregates proved sometimes to be a too large challenge: geopolymerisation occurred too superficially and internally no hardening took place. It was concluded that only the PU aggregates were suitable for the four applications under consideration (blocks, panels, floor screed and floor screed underlay). Together with the PFA as binder the PU aggregates are applicable for blocks, whereas with PFA/GGBS blends as binder they are also applicable for panels and floor screed (underlay) applications although in the latter two cases the workability open time target of 60 minutes could not be guaranteed. It has been mostly the low workability of the mixtures that has limited their application. Contrary to well established cements and aggregates, no suitable additives could be found that were commercially available to improve the workability for the used combination of waste aggregates and binders.

The tested mechanical properties were on average good for all tested mixtures with the exception of the tyre rubber aggregates. Its low compressive strength has been attributed to the low bonding between the aggregates and the matrix. Thermal conductivity was low, as could be expected from the low thermal conductivity values of the aggregates and the (relative) high volume fractions used.

The results show that it is possible to produce a non-structural sustainable concrete with good mechanical and thermal insulation properties that may contribute to a sustainable world.

The numerical concrete mix design method proves to be a very promising tool in designing concrete not only for the compressive strength but also for other performance demands such as elasticity parameters and thermal conductivity. Although there is in general a relation between viscosity of a mix and the workability, the sustainable aggregates combined with the sustainable binders proved to have a low workability, which could not, as yet, be included in the numerical model.

Literature

ACI 211.1-91 (1991). Standard practice for selecting proportions for normal, heavyweight, and mass concrete. *ACI Manual of concrete Practice*, Part 1: Materials and general properties of Concrete, 38 pp, ACI, Detroit, Michigan, USA.

Aliabdo, A. A., Abd Elmoaty, A. E. M., Abd Elbaset, M. M. (2015). Utilization of waste rubber in non-structural applications. *Construction and Building Materials* 91: 195–207.

Al-Sibahy, A., Edwards, R. (2012). Thermal behaviour of novel lightweight concrete at ambient and elevated temperatures: Experimental, modelling and parametric studies. *Construction and Building Materials* 31:, 174–187.

Attanasio, A., Largo, A., Alvarez, I. L., Sonzogni, F., Balaceanu, L. (2015). Sustainable aggregates from secondary materials for innovative lightweight concrete products. *HERON* Vol. 60 (2015) No. 1/2, pp. 5–26.

Banfill, P. F. G. (2006). Rheology of fresh cement and concrete. Rheology Reviews 2006, pp 61–130.

Bentz, D. P. (2005). CEMHYD3D: a three-dimensional cement hydration and microstructure development modeling package. Version 3.0. NISTIR 7232. US Department of Commerce Gaithersburg, MD, USA.

Bernal, S. A., de Gutiérrez, R. M., Pedraza, A. L., Provis, J. L., Rodriguez, E. D., Delvasto, S. (2011). Effect of binder content on the performance of alkali-activated slag concretes. *Cement and Concrete Research* 41(1): 1–8.

Bishnoi, S., Scrivener, K. L. (2009). μic: A new platform for modelling the hydration of cements. *Cement and Concrete Research* 39(4): 266–274.

Blackery, J., Mitsoulis, E. (1997). Creeping motion of a sphere in tubes filled with a Bingham plastic material. *Journal of Non-Newtonian Fluid Mechanics* 70: 59–77.

Brás, A., Leal, M., Faria, P. (2013). Cement-cork mortars for thermal bridges correction. Comparison with cement-EPS mortars performance. *Construction and Building Materials* 49: 315-327.

Bravo, M., de Brito, J. (2012). Concrete made with used tyre aggregate: durability-related performance. *Journal of Cleaner Production* 25: 42–50.

Breugel, K. van (1991*). Simulation of hydration and formation of structure in hardening cement-based materials*. Ph.D. thesis, Delft University of Technology.

Carson, J. K., Lovatt, S. J., Tanner, D. J., Cleland, A. C. (2005). Thermal conductivity bounds for isotropic, porous materials. *International Journal of Heat and Mass Transfer* 48(11): 2150–2158.

Chabra, R., Richardson, J. (2011). Non-Newtonian flow and applied rheology: *engineering applications* (2nd ed.). Butterworth-Heinemann, Oxford, UK.

Choi, Y.-W., Moon, D.-J., Chung, J.-S., Cho, S.-K. (2005). Effects of waste PET bottles aggregate on the properties of concrete. *Cement and Concrete Research* 35(4): 776–781.

Collepardi, M., Collepardi, S., Troli, R. (2007). Concrete mix design. Grafiche Tintoretto, Castrette di Villorba TV, Italy.

Collins, F. G., Sanjayan, J. G. (1999). Workability and mechanical properties of alkali activated slag concrete. *Cement and Concrete Research* 29(3): 455–458.

Eldin, N. N., and Senouci, A. B. (1993). Rubber-tire particles as concrete aggregate. *Journal of Materials in Civil Engineering* 5(4): 478–496.

EuroLigthCon (2007), Grading and Composition of the Aggregate, EuroLight report BE96-3942/R7, Sintef, Norwegen.

Fattuhi, N. I., Clark, L. A. (1996). Cement-based materials containing shredded scrap truck tyre rubber. *Construction and Building Materials* 10(4): 229–236.

Fennis, S. (2011). *Design of ecological concrete by particle packing optimization*. Ph.D. thesis, Delft University of Technology, Delft, The Netherlands.

Fib (2004), Environmental Design. *Fib bulletin 28*, Fib, Lausanne, Switzerland.

Fib (2012), *Model Code for Concrete Structures 2010*, Fib Lausanne, Switzerland.

Fib (2015), *Benchmarking of deemed-to-satisfy provisions in standards*, Fib Lausanne, Switzerland.

Flatt, R. J., Roussel, N., Cheeseman, C. R. (2012). Concrete: An eco material that needs to be improved. *Journal of the European Ceramic Society* 32(11): 2787–2798.

Gijlswijk, R. N. van, Pascale, S., de Vos, S. E., Urbano, G. (2015). Carbon footprint of concrete based on secondary materials. *HERON* Vol. 60 (2015) No. 1/2, pp. 113-142.

He, H. (2010*). Computational modelling of particle packing in concrete*. Ph.D. thesis, Delft University of Technology, Delft, the Netherlands.

He, H., Stroeven, P., Stroeven, M., Sluys, L. J. (2012a). Influence of particle packing on elastic properties of concrete. *Magazine of Concrete Research*. 64 (2): 163-175.

He, H. Le, N.L.B., Stroeven, P. (2012b). Particulate structure and microstructure evolution of concrete investigation by DEM. Part 1: Aggregate and binder packing, *HERON* Vol. 57 (2012) No. 2 , pp. 112–132.

Herrero, S., Mayor, P., Hernández-Olivares, F. (2013). Influence of proportion and particle size gradation of rubber from end-of-life tires on mechanical, thermal and acoustic properties of plaster–rubber mortars. *Materials & Design* 47: 633–642.

Jo, B.-W., Park, S.-K., Kim, C.-H. (2006). Mechanical properties of polyester polymer concrete using recycled polyethylene terephthalate. *ACI Structural Journal* 103(2): 219-225.

Kloss, C., Goniva, C., Hager, A., Amberger, S., Pirkers, S. (2012). Models, algorithms and validation for opensource DEM and CFD–DEM. *Progress in Computational Fluid Dynamics* 12: 140–152.

Kosmatka, S. H., Wilson, M. L. (2011). Design and Control of Concrete Mixtures: The guide to applications, methods, and materials. 15th Editions. PCA, Skokie, Illinois USA.

Lakshmi, R., Nagan, S. (2010). Studies on concrete containing E plastic waste. International *Journal of Environmental Sciences* 1(3): 270–281.

Le L.B.N., Stroeven M, Sluys L.J., Stroeven P. (2013) A novel numerical multi-component model for simulating hydration of cement. *Comput Mater Sci* 78:12–21.

Le, L.B.N., Sluys, L.J., Stroeven M. , Stroeven, P. (2014), Implication of pore structure on micro-mechanical behaviour of virtual cementitious materials, *Computational Modelling of Concrete Structures* (eds. Bicanic *et al.*), Taylor and Francis Group, London pp. 109-116.

Lee, N. K., Lee, H. K. (2013). Setting and mechanical properties of alkali-activated fly ash/slag concrete manufactured at room temperature. *Construction and Building Materials* 47: 1201–1209.

Marzouk, O. Y., Dheilly, R. M., Queneudec, M. (2007). Valorization of post-consumer waste plastic in cementitious concrete composites. *Waste Management* 27(2): 310–318.

Mounanga, P., Gbongbon, W., Poullain, P., Turcry, P. (2008). Proportioning and characterization of lightweight concrete mixtures made with rigid polyurethane foam wastes. *Cement and Concrete Composites* 30(9): 806–814.

Mueller, H.A., Breiner, R., Moffatt, J.S., Haist, M. (2014). *Design and properties of sustainable concrete*. Procedia Engineering 95: 290-304.

Nath, P., Sarker, P. K. (2014). Effect of GGBFS on setting, workability and early strength properties of fly ash geopolymer concrete cured in ambient condition. *Construction and Building Materials* 66: 163–171.

Neville, A.M. (2002). *Properties of Concrete*, 4th edition, Pearson Prentice Hall, Harlow, England.

Ordonez-Miranda, J., Alvarado-Gil, J. J. (2012). Thermal conductivity of nanocomposites with high volume fractions of particles. *Composites Science and Technology* 72(7): 853–857.

Perevozchikov, A., Yakovlev, G., Kodolov, V. (2000). Polyethylene foam waste utilization for light-weight concrete production. *International Journal of Polymeric Materials* 47(1): 7–17.

Petit, J. Y., Wirquin, E., Vanhove, Y., Khayat, K. (2007). Yield stress and viscosity equations for mortars and self-consolidating concrete. *Cement and Concrete Research* 37(5): 655–670.

Pezzi, L., De Luca, P. A., Vuono, D., Chiappetta, F., Nastro, A. (2006). Concrete products with waste's plastic material (bottle, glass, plate). In *Materials Science Forum*, Vol. 514-516 (no. 2): 1753–1757.

Provis, J., and van Deventer, J. (2014). *Alkali Activated Materials*. Springer, The Netherlands.

Rebeiz, K. S. (1996). Precast use of polymer concrete using unsaturated polyester resin based on recycled PET waste. *Construction and Building Materials*, 10(3), 215–220.

Sabnis, G. M. (2011). *Green Building with Concrete: Sustainable Design and Construction*. CRC Press, Boca Raton, USA.

Sikalidis, C. A., Zabaniotou, A. A., Famellos, S. P. (2002). Utilisation of municipal solid wastes for mortar production. *Resources, Conservation and Recycling* 36(2): 155–167.

Stroeven, M. (1999). *Discrete numerical modelling of composite materials-Application to cementitious materials*. Ph.D. thesis, Delft University of Technology, Delft, The Netherlands.

Stroeven, P., Li, K., Le, L.B.N. , Stroeven, M. (2015). Capabilities for property assessment on different levels of the micro-structure of DEM-simulated cementitious materials. *Construction and Building Materials* 88: 105-117.

Sukontasukkul, P., and Chaikaew, C. (2006). Properties of concrete pedestrian block mixed with crumb rubber. *Construction and Building Materials* 20(7): 450–457.

Václavík, V., Dvorský, T., Dirner, V., Daxner, J., Šťastný, M. (2012). Polyurethane foam as aggregate for thermal insulating mortars and lightweight concrete. *Tehnički vjesnik–Technical Gazette* 19(3): 665–672.

Vinai, R., Panagiotopoulou, C., Soutsos, M., Taxiarchou, M., Zervaki, M., Valcke, S., Ligero, V. C., Couto, S., Gupta, A., Pipilikaki, P., Alvarez, I. L., Coelho, D., Branquinho, J. (2015). Sustainable binders for concrete: A structured approach from waste screening to binder composition development. *HERON* Vol. 60 (2015) No. 1/2, pp 27-57.

Visser, J.H.M., Bigaj-van Vliet, A. J., (2014). Designing sustainable concrete on the basis of equivalence performance: assessment criteria for safety. Proc. *4th Intl. FIB congress on Improving Performance of Concrete Structure*. Mumbai, February 10 – 13, 2014, India, pp 1-11.

Wang, X., Wang, K., Han, J., Taylor, P. (2015). Image analysis applications on assessing static stability and flowability of self-consolidating concrete. *Cement and Concrete Composites* 62: 156–167.

Annex Mix compositions

Mix ID	Binder (kg/m³ concrete)	Activators* (kg/m³ concrete)	Aggregate (kg/m³ concrete)	Water (kg/m³ concrete)
2_1	PFA 459	WG 92 NaOH 53	PU foam 4-8 mm 139 normsand 0-2 mm 477	116
2_2	PFA558	WG 112 NaOH 65	PU foam 165	70
2_3	PFA 589	WG 118 NaOH 68 kg	Tyre rubber 0-0.6 mm 49, tyre rubber 2-4 mm 315 normsand 0-2 mm 331	135
2_4	PFA 648 kg	WG 130 NaOH 75	Remix HD 1-4 mm 255 normsand 0-2 mm 358	130
3_1	PFA367 GGBS 122 kg	WG 98 NaOH 38	PU 0-4 mm 52 PU 4-8 mm 97	148
3_2	PFA 481 GGBS 85 g	WG 113 NaOH 66	PU 0-4 mm 74 PU 4-8 mm 74	166
3_3	PFA 76 GGBS 433	WG 112 NaOH 43	PU 0-4 mm 52 PU 4-8 mm 97	149
3_4	PFA 350 GGBS 350	WG 140 NaOH 81	Remix HD 1-4 mm 259 Remix LD 8-12.5 mm 53	171

*) WG: waterglass; NaOH: sodium hydroxide (50%)